LA-UR -85-3389

CONF-860616--4

OCT 09 1985

Los Alamos National Laboratory is operated by the University of California for the United States Department of Energy under contract W-7405-ENG-36

LA-UR--85-3389

DE86 000805

TITLE: TECHNIQUE FOR MEGABAR CONTROLLED STRAIN EXPERIMENTS

AUTHOR(S): Karl P. Staudhammer, MST-7
Kaye A. Johsnon, MST-13

MASTER

SUBMITTED TO: International Symposium on Intense Dynamic Loading and its Effects, Beijing, China June 3-7, 1986

DISTRIBUTION OF THIS DOCUMENT IS UNLIMITED

Los Alamos
Los Alamos National Laboratory
Los Alamos, New Mexico 87545

FORM NO 836 R4
ST NO 2629 5/81

TECHNIQUE FOR MEGABAR CONTROLLED STRAIN EXPERIMENTS

K. P. Staudhammer
K. A. Johnson
Materials Science and Technology Division
Los Alamos National Laboratory
Los Alamos, NM 87545

Many shock recovery experimenters have tended to plot material effects vs pressure or calculated pressure. [1-4] Different experimental designs (and design variations in trapping and latteral supports) can result in significant variations in strain and stress state in the differing designs. [5,6] While design is perhaps of lesser importance to measurements made during the shock, analysis and plotting residual effects versus pressure rather than to strain may have lead to misinterpretation. Many of the properties that are measured are indeed shock induced, but among the pertinent variables are the shock induced strain not the pressure per se. Since in most designs the variation in strain appears to be nominally inversely proportional to the trapping and lateral support, we propose that most shock loading effects are reflected tensile wave results and have very little to do with the initial shock wave. Indeed it might be conjectured that with perfect trapping we might have no macro-residual effects at all. Most of the well controlled recovery studies have been flyer plate experiments. [7,8] Due to the inherent nature of the flyer plate design, the amount of the strain has been very closely aligned/related to the intrinsic nature of the experiment. Thus for most flyer plate experiments, increasing pressure, explosives, and flyer plate mass, results in an increased amount of strain (as well as residual temperature). This builds a fortuitous correlation into flyer plate experiments.

This series of designs and variations on a design presented here can semi-independently evaluate shock effects of residual strain vs variations in pressure. These variations in effects are, in fact, reflected tensile wave effects. The strain rate is, however, equivalent to the shock wave itself and they are 10^6/s effects.

Residual temperatures are another important shock effect which can significantly affect recovery microstructures and properties. The residual temperature in practical experiments is a sum of the entropic and strain heats and not directly related to the pressure. [9] The published data [10] on residual temperature do not take the magnitude of strain into account and such tables should only be referred to with caution as minimums. At best, these temperature data should be applied only as a minimal guide.

Experimental

Figure 1 illustrates the cylindrical arrangement for subjecting a sample (solid or powder holder) to continuously varying pressure along the specimen axis length from 12 to 170 GPa. [5] For this arrangement, detonation of the main charge (composition C-4 explosive) begins radially at the top edge of the specimen and as the detonation wave moves radially outward and downward, the pressure is added incrementally at a rapid rate (∿ 8 km/s). The pressure profile along the specimen as well as within is obtained from a two-dimensional Eulerian computer code in use at Los Alamos National Laboratory. This code can produce complete shock wave profiles at any instant of time (axial distance and radius) from the initiation of detonation so that maximum pressure at any point along an axial reference of the specimen can be determined. Such a profile for the outer radius and the central axis are shown in Figure 2. The maximum pressure of 170 GPa is achieved approximately 2/3 of the distance from the top of the specimen. The samples were solid annealed 304L stainless steel. The configuration is shown schematically in Figure 1. The dimensions were 63.4 mm in length and 38.1 mm in diameter. The cylinders were split in half to facilitate strain measurements. One anvil face of the solid specimen cylinder was electrolytically plated with a thin copper circle grid in order to monitor local strain by measuring the circle shape changes. Using this technique strains could be measured to 1% accuracy. Specific strain values in the shocked samples are obtained by varying the momentum trap thickness (i.e. top and bottom plates).

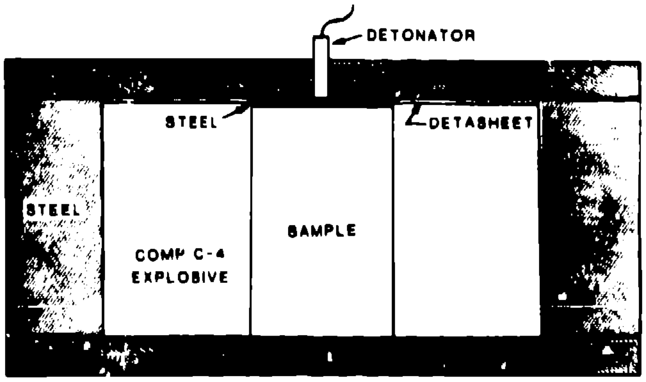

Figure 1 Cylindrical implosion assembly schematic.

Results

As shown in Figure 3 the greater the momentum trap thickness the lower the overall strain. Momentum traps greater than 5 cm were not beneficial in reducing overall strain. The two data points with low strain were from a pedestal design illustrated in Figure 4. All strains plotted in Figure 3 are for overall sample strains. Peak local strain which occurs at the specimen bottom is approximately twice the overall strain. The thickness as plotted includes the 2.5 cm pedestal height. The pedestal insures that the shock wave has exited the sample prior to the detonation front impinging on the bottom trap.

Further evidence that the strain in these designs is caused primarily by reflected tensile waves is shown in Figure 6. The localized strain values from one experiment are plotted for both axial and radial measurements. The linear nature fits neither the axial pressure ramp-up or the steady state outer diameter pressure and suggests an attenuating reflected tensile wave.

The pressure profile as generated by the 2-D Eulerian code is essentially independent of the resulting residual strain. Consequently, microstructural changes that are observed, are due, in large

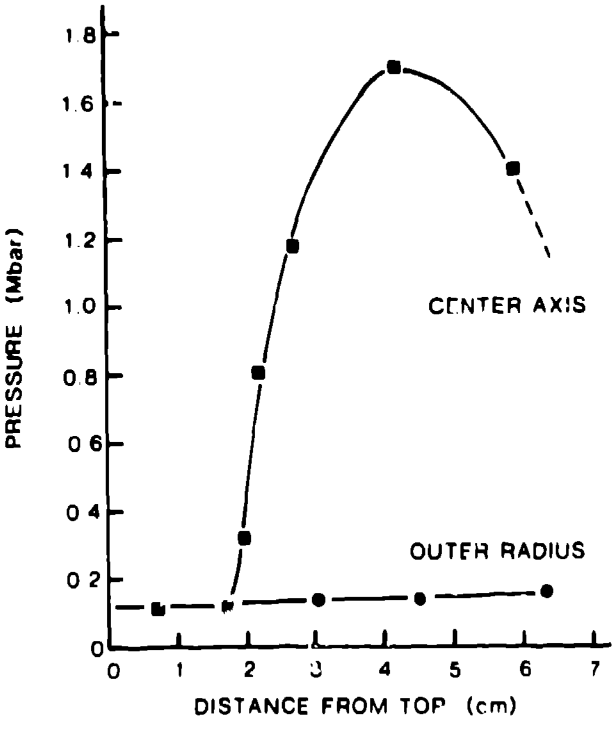

Figure 2 Calculated pressure versus distance in 304 stainless steel along central axis and outer radius of the test specimen.

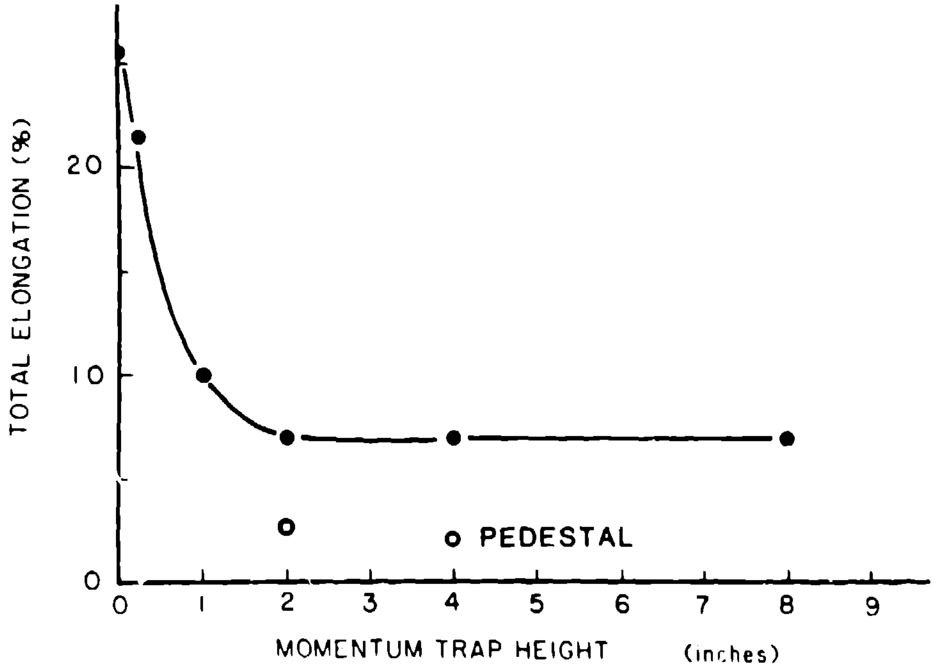

Figure 3 Overall strain versus momentum trap height including pedestal design for 304 stainless steel.

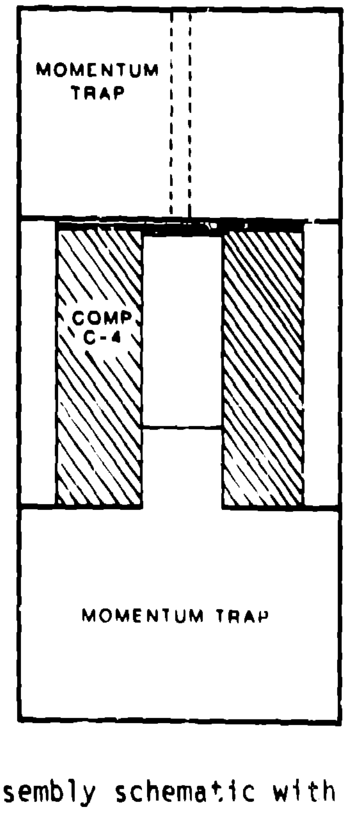

Figure 4 Cylindrical assembly schematic with pedestal trap.

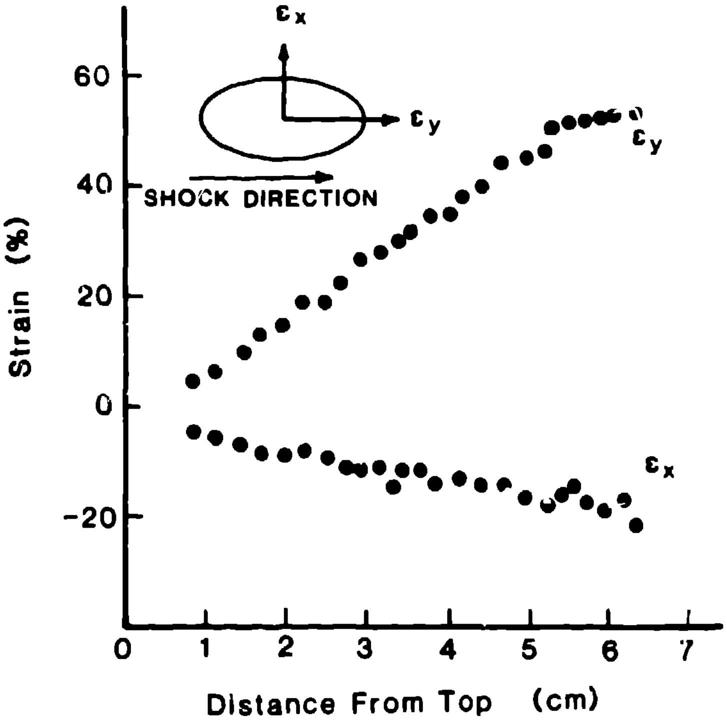

Figure 5 Distance versus residual strain along the central axis of a 170 GPa shocked sample using a 7.6 cm momentum trap.

part to strain. Conventional momentum trap design as shown in Figure 1, are limited in strain reduction to approximately 6% (12% maximum local strain) as shown in Figure 4, if sufficient momentum trap height is used. An experimental goal was to isolate the strain component of the shock effect. To this degree the sample interface/pedestal design was initiated. With this design the overall strain was reduced to 2% (4% maximum, localized). This low strain design offers an opportunity to study shock effects and has significant implications for cylindrical compaction of brittle materials including ceramics. For example, ceramic compaction work using this equivalent design [11] with a short trap height resulted in numerous cracks of the consolidated powder. This is not surprising since the sample holder was strained to 22% resulting from the 0.64 cm thick momentum traps. A far better compact might be achieved with a 10 cm pedestal design.

Conclusions

1. This design allows in one shot one experiment a range of pressures from 12-170 GPa and a selectable strain range (0 to 55%) in 304 stainless steel with 100% recovery.

2. Development of the application of griding has enabled correlation, locally, of pressure and strain with structure and properties at a strain rate of 10^6/s.
3. Appropriate variations in momentum trap design can control strain in cylindrical implosion shock experiments.
4. Pedestal type traps have shown significant improvement in the reduction of strain in cylindrical implosion experiments. Such design would seem to be appropriate for experiments on brittle and ceramic materials.
5. In cylindrical designs the degree of macro-strain is a function of trapping and is the result of reflected waves not the primary shock pulse.

Acknowledgement

The authors wish to acknowledge A. D. Bonner for the explosive and firing site assistance.

References

[1] Murr, L. E., "Shock Waves and High-Strain-Rate Phenomena in Metals", M. A. Meyers and L. E. Murr, ed. Plenum Press (1981) p 753.
[2] Meyers, M. A., Mater. Sci., Engr. 30, (1977) p 99.
[3] Leslie, W. C., "Proc. Conf. on Metallurgical Effects at High Strain Rates", Rohde, R. W. Butcher, B. M. Holland, J. R. and Karnes, C. H. (eds), Plenum Press, New York, (1973) p 571.
[4] Duvall, G. E., Bellamy, P. M., Livak, R. J., "Shock Waves and High-Strain-Rate Phenomena in Metals", M. A. Meyers and L. E. Murr, ed. Plenum Press (1981) p. 717.
[5] Staudhammer, K. P., Johnson, K. A., Olinger, B., "Shock Waves In Condensed Matter", Asay, J. R., Graham, R. A., Straub, G. K., ed. Elsiver Science Pub. B. V., (1983) p 419.
[6] Johnson, K. A., Murr, L. E., Staudhammer, K. P., Acta Metall Vol. 33, No. 4, (1985) p 677.
[7] Murr, L. E., "Shock Waves and High-Strain-Rate Phenomena in Metals", M. A. Meyers and L. E. Murr, ed. Plenum Press, (1981) Chapter 37.
[8] Clifton, R. J., "Shock Waves In Condensed Matter", Assay, J. R., Graham, R. A., Straub, G. K., ed. Elsiver Science Pub. B. V. (1983) p 105.
[9] Johnson, K. A., Staudhammer, K. P., "EXPLOMET 85", L. E. Murr, K. P. Staudhammer and M. A. Meyers, ed., Marcel Dekker, March 1986.
[10] McQueen, R. G., et.al., "Shock Waves and High-Strain-Rate Phenomena in Metals", M. A. Meyers and L. E. Murr, ed. Plenum Press, (1980) Appendix B.
[11] Petrovic, J. J., Olinger, B. W., Roof, R. B., "Shock Waves In Condensed Matter", Asay, J. R., Graham, R. A., Straub, G. K., ed. Elsiver Science Pub. B. V., (1983) p 463.